IMPROVING THERMAL PERFORMANCE OF MICRO-CHANNEL ELECTRONIC HEAT SINK USING SUPERCRITICAL CO_2 AS COOLANT

by

Jahar SARKAR

Department of Mechanical Engineering, Indian Institute of Technology (B. H. U.), Varanasi, India

Original scientific paper
https://doi.org/10.2298/TSCI161110030S

In view of increasing tendency of power density of electronic systems, cooling performance improvement of micro-channel heat sink is an emerging issue. In the present article, supercritical CO_2 is proposed as a heat transfer fluid in micro-channel heat sink for power electronics cooling. Energetic and exergetic performance analyses of micro-channel heat sink using supercritical CO_2 have been done and compared with conventional coolant, water. To take care of sharp change in properties in near critical region, the discretization technique has been used for simulation. Effects of both operating and geometric parameters (heat flux, flow rate, fluid inlet temperature, channel width ratio, and channel numbers) on thermal resistance, heat source (chip) temperature, pressure drop, pumping power and entropy generation are presented. Study shows that the thermal resistance, heat source temperature and pumping power are highly dependent on CO_2 inlet pressure and temperature. Supercritical CO_2 yields better performance than water for certain range of fluid inlet temperature. For the studied ranges, maximum reduction of thermal resistance by using CO_2 is evaluated as 30%. Present study reveals that there is an opportunity to use supercritical CO_2 as coolant for power electronic cooling at lower ambient temperature.

Key words: *supercritical CO_2, micro-channel heat sink, electronics cooling*

Introduction

The conventional cooling technologies, including natural air convection and forced air convection, have become hard to cool the high heat flux ($\geq$100 W/cm^2) in high power electronic applications: such as, integrated power electronics module (IPEM). The two important objectives in electronics cooling – minimization of the maximum substrate temperature and reduction of substrate temperature gradients – can be achieved by the use of liquid-cooled micro-channels. The micro-channel heat sink (MCHS) exhibits great potential in power electronics cooling since the first fabrication by Tuckerman and Pease [1], which cooled a heat flux of 790 W/cm^2 with a temperature rise of 71 °C. This landmark has activated great interests in application of MCHS for electronics cooling and many subsequent R&D works [2] have been done to make it as one of the most efficient technologies for high power electronics applications.

Within last three decades, large numbers of research and development activities have been done on MCHS, including heat transfer and pressure drop characteristics [3, 4], effects of fluid property variation [5], the importance of scaling effects of fluid-flow [6], and dimensional optimization [7]. In general, there are two options for performance improvement of MCHS:

Author's e-mail: jsarkar.mec@itbhu.ac.in

material and design optimization of MCHS and use of suitable heat transfer fluid. Use of suitable heat transfer liquid should fulfill several criteria such as, performance, operating range, thermal and chemical stability, *etc*. Water was initially proposed as heat transfer fluid and it is still best choice for electronics applications. Apart from this, ethylene glycol-water brine, methanol-water mixture, FC-72, *etc*., were also proposed. Recently, nanofluids also have been proposed as heat transfer fluid and lots of numerical and experimental works for nanofluid-cooled MCHS have been conducted [8-14]. In the present study, supercritical CO_2 is being proposed as a heat transfer fluid in MCHS for electronics cooling.

Recently, the CO_2 has been emerged as working substance for various engineering applications. Apart from its easy availability, environmental friendliness and personal safety natures, supercritical CO_2 yields excellent thermophysical properties. Hence, the CO_2 has been revived as a suitable refrigerant for various refrigeration and air-conditioning devices [15, 16]. Apart from this, it has been emerged as working substance in supercritical Brayton cycle for next generation nuclear reactor and solar applications [17]. It has been also proposed working fluid for supercritical Rankine power cycle for the utilization of low grade heat [18]. Recently, the supercritical CO_2 has been proposed as heat transmission fluid for geothermal heat extraction [19], solar thermal collector [20], and many other applications [21-25]. However, to the best of the authors' knowledge, no study on MCHS has been conducted by using supercritical CO_2 as a coolant for electronic cooling.

In this study, the energetic as well as exergetic performance analyses of MCHS using supercritical CO_2 have been conducted for electronic applications and compared with conventional coolant, water. To take care of the sharp change in thermophysical and transport properties in near critical region, the discretisation technique has been used for simulation of MCHS. Effects of heat flux, fluid inlet temperature, fluid mass-flow rate and channel geometry (channel with ratio, number of channels, and aspect ratio) on chip temperature, thermal resistance, pumping power (PP), and entropy generation are presented.

Mathematical modeling and simulation

The cooling circuit of a high power integrated circuit (IC) chip is shown in fig. 1 [8]. A MCHS, fig. 2, is used to extract heat generated in chip and a heat exchanger (gas cooler) is used to reject heat to the ambient. The coolant flows through parallel rectangular channels of heat sink, fig. 2, and is acted as a heat transmission fluid between heat sink and heat exchanger. A pump is used to maintain required pressure rise for flow through MCHS – heat exchanger system. Single layered MCHS structure [14] is considered in this study and supercritical CO_2 is proposed as a coolant. As the main aim of this study to promote supercritical CO_2 as coolant in MCHS, the performance of MCHS using supercritical CO_2 has been only studied. The following assumptions have been made for the analysis:

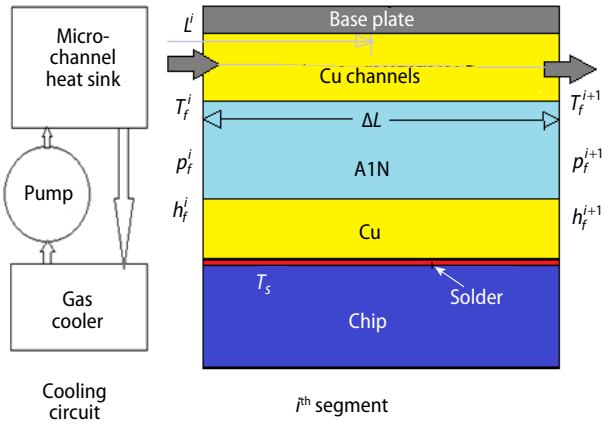

Figure 1. Cooling circuit and a computational segment

– Single-phase, both heat transfer and fluid-flow are in steady state.
– The effects of natural convection and radiation are neglected.
– Heat generation through chip surface is uniform.
– Coolant is equally distributed through channels and both heat transfer and fluid-flow characteristics in each channel are identical (only varying with channel length).

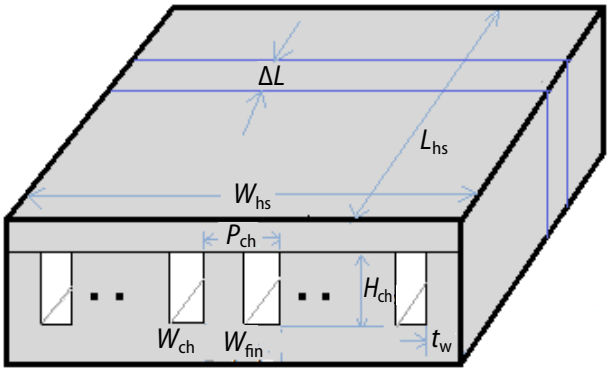

Figure 2. Micro-channel configuration and dimensions

It may be noted that properties of CO_2 changes abruptly near the critical point. To consider the lengthwise property variation, the MCHS has been discretised, and momentum, energy and entropy balance equations have been applied to each segment.

For given channel width ratio and number of flow channels, channel pitch, channel width and fin thickness can be calculated by:

$$P_{\mathrm{ch}} = \frac{W_{\mathrm{hs}} - 2t_{\mathrm{w}}}{N_c + \beta - 1}, \quad W_{\mathrm{ch}} = \beta P_{\mathrm{ch}}, \quad W_{\mathrm{fin}} = (1-\beta) P_{\mathrm{ch}} \tag{1}$$

The MCHS has been divided lengthwise into number of small segments of length, ΔL, as shown in fig. 2. Applying energy balance at i^{th} computational segment:

$$\dot{m}_f (h_f^{i+1} - h_f^i) = \dot{Q}^i = W_{\mathrm{hs}} \Delta L q'' \tag{2}$$

$$\frac{T_s^i - T_f^i}{R_{\mathrm{tot}}} = \dot{Q}^i = W_{\mathrm{hs}} \Delta L q'' \tag{3}$$

Assuming that the heat generated in chip is absorbed by coolant only and neglecting thermal resistance of solder, the total thermal resistance of a segment is consist of conductive thermal resistances of copper and AlN layers, convective thermal resistance and capacitive thermal resistance. Hence:

$$R_{\mathrm{tot}} = R_{\mathrm{Cu}} + R_{\mathrm{AlN}} + R_{\mathrm{conv}} + R_{\mathrm{cap}} = \frac{t_{\mathrm{Cu}}}{k_{\mathrm{Cu}} W_{\mathrm{hs}} \Delta L} + \frac{t_{\mathrm{AlN}}}{k_{\mathrm{AlN}} W_{\mathrm{hs}} \Delta L} + \frac{1}{\eta_0 \alpha_f A_{\mathrm{eff}}} + \frac{1}{2 \dot{m}_f c_{pf}} \tag{4}$$

Here, product of effective area and overall fin efficiency is given [2, 13]:

$$\eta_0 A_{\mathrm{eff}} = N_c \left[W_{\mathrm{ch}} + 2 H_{\mathrm{ch}} \eta_{\mathrm{fin}} \right] \Delta L \tag{5}$$

where fin efficiency, η_{fin} is given [2]:

$$\eta_{\mathrm{fin}} = \frac{\tanh(m H_{\mathrm{ch}})}{m H_{\mathrm{ch}}}, \quad m = \sqrt{\frac{2\alpha_f}{k_{\mathrm{Cu}} W_{\mathrm{fin}}}} \tag{6}$$

The coolant heat transfer coefficient in a segment is given:

$$\alpha_f = \frac{\mathrm{Nu}\, k_f}{D_h} \tag{7}$$

No correlation is available particularly for supercritical CO_2 heating in rectangular micro-channel. Many studies (*e. g.* [23]) showed that single-phase correlation can be applied for supercritical CO_2 also. Ducoulombier *et al.* [26] used Hausen correlation (widely used for laminar flow with entrance effect) for supercritical CO_2 cooling in circular micro-channel. Hence, Hausen correlation applicable for rectangular channel with four sides heated [13] has been used. Therefore, the average Nusselt number of a segment is given [13]:

$$\mathrm{Nu} = \mathrm{Nu}_\infty + \frac{0.14\,\mathrm{Gz}}{1 + 0.05\mathrm{Gz}^{2/3}} \tag{8}$$

where the Nusselt number for the fully developed laminar flow is given by (Re < 2200) [13]:

$$\mathrm{Nu}_\infty = 8.235\left(1 - \frac{2.0421}{Ar} + \frac{3.0853}{Ar^2} - \frac{2.4765}{Ar^3} + \frac{1.0578}{Ar^4} - \frac{0.1861}{Ar^5}\right) \tag{9}$$

The dimensionless Graetz number determines the importance of entrance effect which should be taken into account when Gz > 10:

$$\mathrm{Gz} = \frac{\mathrm{Re}\,\mathrm{Pr}\,D_h}{L^i}, \quad L^i = \left(i - 1 + \frac{i}{2}\right)\Delta L \tag{10}$$

The pressure drop in a segment is given [4]:

$$p_f^i - p_f^{i+1} = \Delta p_f = \frac{\left(\dfrac{\dot{m}_f}{N_c}\right)^2}{2\rho_f {A_c}^2} 4 f_{\mathrm{app}} \frac{\Delta L}{D_h} \tag{11}$$

where apparent Fanning friction factor is expressed as (Re < 2300, Ar < 10) [4]:

$$f_{\mathrm{app}} = \frac{1}{\mathrm{Re}}\left\{\left[3.2\left(\frac{\mathrm{Re}\,D_h}{\Delta L}\right)^{0.57}\right]^2 + \left[4.7 + 19.64\frac{Ar^2 + 1}{(Ar+1)^2}\right]^2\right\}^{0.5} \tag{12}$$

The pressure drop across the heat sink consists of three parts: the pressure drop across the flow channels, the pressure drop at the inlet due to the flow constriction and at the exit due to the flow expansion. Hence:

$$\Delta p_{\mathrm{tot}} = \sum \Delta p_{\mathrm{segment}} + \frac{\left(\dfrac{\dot{m}_f}{N_c}\right)^2}{2\rho_f {A_c}^2} K \tag{13}$$

where the loss coefficient, K, at inlet and outlet of heat sink is given [2]:

$$K = 0.6\left(\frac{N_c A_c}{W_{hc} H_{ch}}\right)^2 - 2.4\frac{N_c A_c}{W_{hc} H_{ch}} + 1.8 \tag{14}$$

Hence, the PP is calculated:

$$PP = \frac{\dot{m}_f}{\rho_{f,\mathrm{inlet}}} \frac{\Delta p_{\mathrm{tot}}}{\eta_{\mathrm{pump}}} \tag{15}$$

The overall thermal resistance is expressed:

$$R_{th,hs} = \frac{T_s - T_{f,\text{inlet}}}{\sum_i \dot{Q}_i} \tag{16}$$

The entropy generation in the heat sink can be calculated:

$$\dot{S}_{\text{gen}} = \dot{m}_f \left[(s_{f,\text{exit}} - s_{f,\text{inlet}}) - \frac{(h_{f,\text{exit}} - h_{f,\text{inlet}})}{T_s} \right] \tag{17}$$

A computer (FORTRAN) code has been developed to simulate the MCHS using water and supercritical CO_2 as coolants for various geometry and operating parameters. The temperature dependent correlations available in open literatures [13] have been used for thermophysical properties of water and the previously developed property code CO2PROP [27] is used for thermodynamic and transport properties of supercritical CO_2. Property variation is very abrupt near the critical region and the MCHS encompasses this region. To consider this variation, the entire length of the MCHS has been divided equally into several discrete segments and in each segment, heat transfer coefficient for CO_2 is calculated based on mean values. This way, the MCHS is made equivalent to a number of MCHS arranged in series and the combined heat transfer of all the segments is the total heat transfer of the MCHS. Therefore, fast changing properties of supercritical CO_2 have been modelled accurately in the MCHS. For given heat flux, dimensions and fluid inlet temperature, the followings are calculation steps for each segment: total resistance, eqs. (1), (4)-(10), source temperature and fluid exit temperature, eqs. (2)-(3), and pressure drop, eqs. (11) and (12). Then the heat sink performance parameters, eqs. (13)-(17) and average chip temperature has been calculated. The grid dependent test has showed that the result becomes nearly independent on number of segments (*e. g.* error in fluid exit temperature is less than 0.1% per segment) for number of segments above 15. Hence, the number of segment has been taken as 20 for simulation to confirm accuracy.

Results and discussion

Suitability of using supercritical CO_2 as heat transmission fluid in single-layered single-sided MCHS is examined in this study for power electronics cooling. Following dimensions are considered [13]: length and width of heat sink are 10 mm both, thickness of Cu layer is 300 μm, thickness of AlN is 635 μm and channel height is 300 μm. Thermal conductivities of Cu and AlN are 387.6 W/mK and 180 W/mK, respectively [13]. The CO_2 pressure is taken as 75 bar and to sustain this high pressure, thicker side wall of 0.3 mm has taken (no restriction has been used for internal fin thickness due to similar pressure in both sides). Unless otherwise stated, channel number, and fluid inlet temperature have been taken as 100 and 30 °C, respectively.

To the best of authors' knowledge, no previous result is available in open literature for MCHS with supercritical CO_2. Hence, the code has been quantitatively validated with the experimental data given in [13] for water. Comparison has been done for channel number of 100, channel height of 287 μm, channel width of 55 μm, fin width of 45 μm, which will yield channel width ratio of 0.55 and aspect ratio of 5.22. For inlet water temperature of 297 K, inlet water velocity of 2 m/s and heat flux of 277 W/cm^2, the experimental and simulation values of thermal resistance reported [13] are 0.113 K/W and 0.105 K/W, respectively, whereas, the present simulation code yield the value of 0.109 K/W. Hence, the present code is under-predicted

about 4% from experimental data and this better matching is due to discretization. The various performance parameters of electronic MCHS are exhibited graphically as elucidated below.

Figures 3 and 4 show the variations of thermal resistance and PP with channel width ratio for constant fluid mass-flow rate of 0.001 kg/s and number of channels of 100, respectively (Reynolds number varies from 575 to 1745 and increases lengthwise). For given constant mass-flow rate, with the increase in width ratio, R_{cap}, remains constant and R_{conv} increases due to dual effects of decrease in heat transfer coefficient (as Reynolds number decreases due to decrease in mass velocity) and insignificant increase in surface area, and hence thermal resistance increases monotonically. Whereas, the pressure drop as well as PP decreases due to increase in hydraulic diameter for nearly constant volume flow rate. However, for given constant inlet velocity, the mass-flow rate increases and hence R_{cap} monotonically decreases with increase in channel width ratio, whereas, the heat transfer coefficient decreases due to increase in hydraulic diameter (as the heat transfer coefficient is inversely proportional to hydraulic diameter) and effective area increases insignificantly, and hence as a result, R_{conv} increases. Due to this dual effect of R_{cap} and R_{conv}, the thermal resistance decreases initially and after reaching some minimum value, again increases with increase in channel width ratio and yield some optimum value corresponding to minimum resistance. Thus, the optimal resistance is a trade-off between the heat transfer area and the channel flow resistance. As shown in fig. 4, the optimum channel width ratio is 0.7 for water (similar to previous studies), whereas, 0.75 for CO_2. As shown, the PP insignificantly decreases because the increase of channel cross-section area and decrease of Poiseuille number. Practically, maintaining constant mass-flow rate is easier than constant inlet velocity of channel.

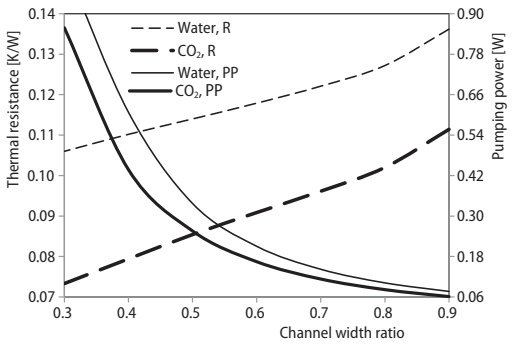

Figure 3. Effect of channel width ratio for constant mass-flow rate

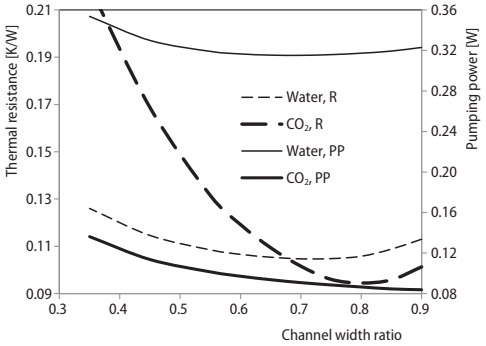

Figure 4. Effect of channel width ratio for constant inlet velocity

Figures 5-9 show the variations of average heat source (chip) temperature, thermal resistance, pressure drop, PP and entropy generation with number of channels by using supercritical CO_2 for channel width ratio of 0.75 and mass-flow rate of 0.001 kg/s for various heat flux conditions (Reynolds number varies from 427 to 2219). With N_c increasing, R_{cap} keeps independent due to constant mass-flow rate, whereas, R_{conv} decreases due to continuous increase in both heat transfer coefficient (decrease in hydraulic diameter) and effective heat transfer area, and hence thermal resistance decreases monotonically, fig. 6. Hence, the overall temperature deference decreases due to constant heat transfer rate and hence source temperature decreases with increase in N_c, fig. 4. On the other hand, the mass-flow rate per channel decreases as well as the cross-section area of a channel also decreases. Hence, as the second effect is more predominant than first one, the pressure drop as well as PP increases due to

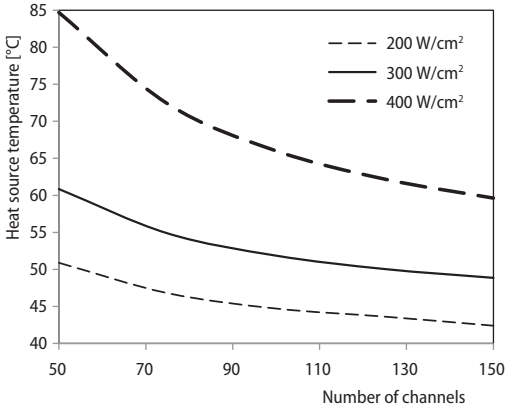

Figure 5. Effect of channel number on heat source temperature

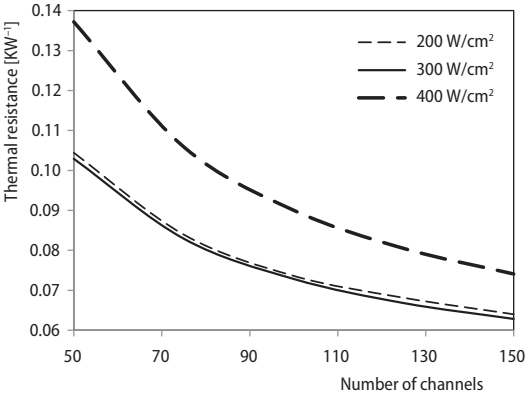

Figure 6. Effect of channel number on thermal resistance

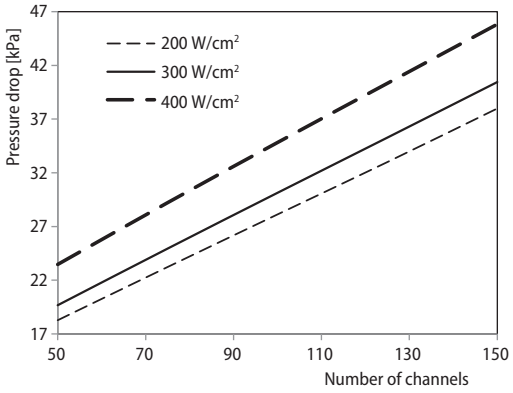

Figure 7. Effect of channel number on channel pressure drop

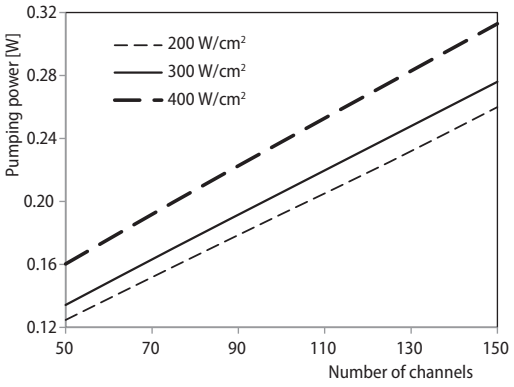

Figure 8. Effect of channel number on pumping power

decrease in mass velocity with increasing N_c. Entropy generation occurs due to thermal resistance (temperature difference) and flow resistance (pressure drop). Here, entropy generation due to thermal resistance decreases and entropy generation due to flow resistance increases with increasing N_c. As the first part is more predominant, total entropy generation decrease with increase in N_c. As the overall dimensions and mass-flow rate are same, it is obvious that both thermal resistance and the heat source temperature and hence entropy generation will be more for higher heat flux. Whereas, the differences in pressure drop and PP with variation of heat flux are mainly due to property variation associated with change in operating condition. Figure 10 shows the performance characteristic curve (thermal resistance *vs.* PP). The thermal resistance decreases rapidly with the PP and then tended to reach a saturated. As discussed, it seems to be always desirable to increase N_c for decrease in thermal resistance. However, the extremely large pressure drop for high N_c makes it impractical to further increase the channel number after a critical value, hence, some trade-off between these two parameters are needed to optimize the channel numbers. As shown in fig. 9, optimum channel number should be in the range of 90 to 100 as the decrease in entropy generation is negligible thereafter.

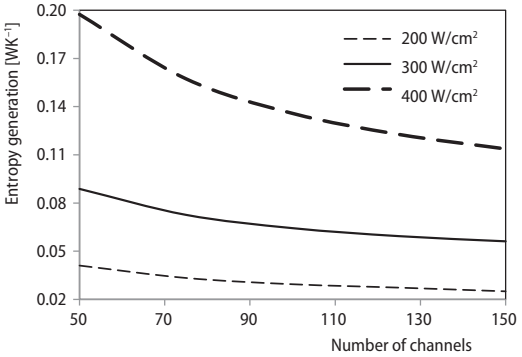

Figure 9. Effect of channel number on entropy generation

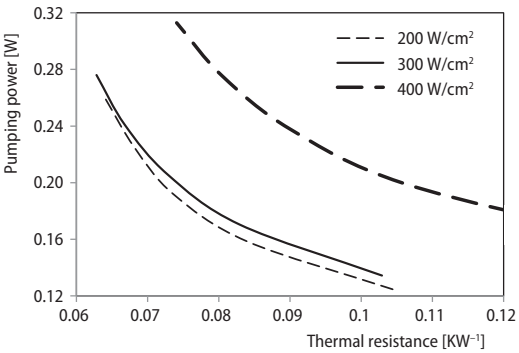

Figure 10. Variation of pumping power with thermal resistance

Performance comparison of supercritical CO_2 with water is shown in tab. 1. As the property variation of water in negligible, the thermal resistance is nearly constant and hence the heat source temperature is only dependent on heat flux and inlet temperature. Whereas, the thermal resistance for supercritical CO_2 is highly dependent on CO_2 inlet pressure as well as

Table 1. Performance comparison ($\dot{m}_f$ = 0.001 kg/s, N_c = 100, β = 0.75)

Coolant	$\tilde{q}$ [Wcm^{-2}]	$T_{f,\text{inlet}}$ [°C]	T_s [°C]	$R_{\text{th,hs}}$ [KW^{-1}]	PP [W]	$\frac{\sum_i \dot{Q}_i}{PP}$	$\dot{S}_{\text{gen}}$ [WK^{-1}]
Water	200	20	44.6	0.1226	0.163	1225	0.0352
	200	30	54.5	0.1221	0.143	1401	0.0328
	300	20	56.8	0.1223	0.154	1947	0.0747
	300	30	66.7	0.1219	0.136	2206	0.0698
Supercritical CO_2	200	20	55.2	0.1755	0.068	2955	0.0566
	200	30	45.1	0.0751	0.095	2101	0.0446
	300	20	58.9	0.1353	0.069	4347	0.0971
	300	30	60.7	0.0961	0.113	2648	0.0937

temperature due to abrupt change in thermophysical and transport properties. Reynolds number for supercritical CO_2 is about 10-12 times more than water and increases significantly along the channel length due to decrease in viscosity. Hence, the heat source temperature is a strong function of fluid pressure, temperature and heat flux. Similar explanation is applicable for pumping power also and pumping power of supercritical CO_2 is lower due to lower viscosity. Hence, performance index (ratio of heat transfer rate to pumping power) is higher for supercritical CO_2. Due to lower temperature rise, the overall temperature difference between heat source and fluid is more for supercritical CO_2, which leads to higher entropy generation rate compared to water. Interestingly, the thermal resistance for CO_2 is higher at 20 °C and lower at 30 °C, which can be detailed illustrated in fig. 11. As shown, the supercritical CO_2 can give better performance than water for inlet temperature higher than 22 °C and maximum reduction of thermal resistance is evaluated as 22% for inlet temperature of 29 °C. Hence, the superiority of supercritical CO_2 as coolant in MCHS for electronic cooling can be observed for certain range of fluid inlet temperatures, which is dependent on heat flux, flow rate and geometry. At near critical operation, CO_2 is better as it exhibits superior thermophysical and transport properties (such as very high

specific heat capacity and thermal conductivity, and lower viscosity) than water (however, water is better in most of the operating conditions). Supercritical CO_2 can be used for the inlet temperature up to critical temperature (≈31 °C) only.

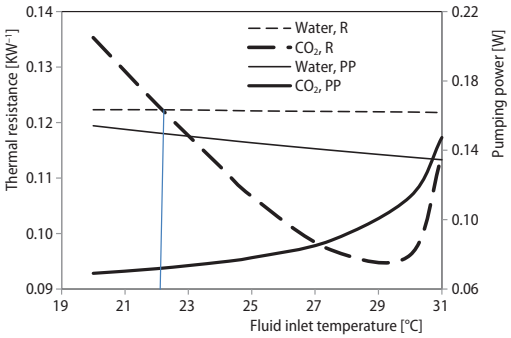

Figure 11. Effect of fluid inlet temperature for heat flux of 300 W/cm^2

Conclusions

Energetic as well as exergetic performance analyses of MCHS using supercritical CO_2 have been done to study effects of various operating and design parameters for electronic applications and compared with water. For given fluid inlet temperature and mass-flow rate, the thermal resistance increases with increase in channel width ratio. However, for given fluid inlet temperature and inlet velocity, the thermal resistance yields some minimum value at optimum channel width ratio. The optimum channel width ratio is 0.7 for water whereas, 0.75 for supercritical CO_2. Result shows that the pumping power requirement decreases with increase in channel width ratio. Variation with number of channels shows that with channel number increasing, thermal resistance decreases and hence source temperature decreases, pressure drop as well as pumping power increases and entropy generation decreases. Both thermal resistance and the heat source temperature and hence entropy generation will be more for higher heat flux. Whereas, the difference in pressure drop and pumping power with variation of heat flux are mainly due to property variation associated with change in operating condition. The thermal resistance decreased rapidly with the pumping power and then tended to reach a saturated and hence, some trade-off between these two parameters is needed to optimize the channel numbers.

Dissimilar to water, due to abrupt change in supercritical CO_2 properties, the thermal resistance and pumping power is highly dependent on CO_2 inlet pressure and temperature. Hence, the heat source temperature is a strong function of fluid pressure, temperature and heat flux. Results show that the MCHS with supercritical CO_2 yields lower thermal resistance compared to water for certain range of fluid inlet temperature (*i. e.* for heat flux of 300 W/cm^2 and flow rate of 0.001 kg/s, CO_2 can give better performance for the minimum inlet temperature of 22 °C). However, CO_2 can be used for the inlet temperature up to critical temperature (≈31 °C) only. For the studied ranges, the maximum reduction of thermal resistance upto 30% can be achieved for optimum inlet temperature. Study shows that supercritical CO_2 is suitable for lower ambient temperature as heat transmission fluid in MCHS for electronic cooling.

Nomenclature

Ac – channel cross-sectional area
Ar – channel aspect ratio, (= H_{ch}/W_{ch}), [–]
c_{pf} – fluid specific heat capacity, [Jkg^{-1}K^{-1}]
D_h – channel hydraulic diameter, [m]
Gz – Graetz number, [–]
H_{ch} – channel height, [mm]
h_f – fluid specific enthalpy, [Jkg^{-1}]
k_{Cu}, k_{AlN} – thermal conductivity, [W/m^{-1}K^{-1}]
k_f – fluid thermal conductivity, [Wm^{-1}K^{-1}]
L_{hs} – heat sink or channel length, [mm]
ΔL – segmental length, [mm]
$\dot{m}_f$ – fluid mass-flow rate, [kgs^{-1}]
N_c – number of micro-channels
Nu – Nusselt number, [–]
P_{ch} – channel pitch, [mm]
p_f – fluid pressure, [kPa]
PP – pumping power, [W]
Pr – Prandtl number, [–]
$\dot{Q}$ – heat transfer rate, [W]
q'' – heat flux, [Wcm^{-2}]

R_{cap} – capacitive thermal resistance, [KW^{-1}]
R_{conv} – convective thermal resistance, [KW^{-1}]
R_{Cu}, R_{AlN} – conductive thermal resistance, [KW^{-1}]
Re – Reynolds number, [–]
$\dot{S}$ – specific entropy, [Jkg^{-1}K^{-1}]
t_{Cu}, t_{AlN} – thickness of interfacial layer, [mm]
t_w – side wall thickness, [mm]
T_f – fluid temperature, [°C]
T_s – chip temperature, [°C]
W_{ch} – channel width, [mm]
W_{fin} – fin width or thickness, [mm]
W_{hs} – heat sink width, [mm]

Greek symbols

α_f – heat transfer coefficient, [Wm^{-2}K^{-1}]
β – channel width ratio, (= W_{ch}/P_{ch}), [–]
η_0 – overall fin efficiency
η_{pump} – pump efficiency
ρ_f – fluid density, [kgm^{-3}]

Acronyms

AlN – aluminum nitride nanoparticle

References

[1] Tuckerman, D. B., Pease, R. F., High Performance Heat Sinking for VLAI, *IEEE Electron. Devices Letter*, EDL-2 (1981), 5, pp. 126-129
[2] Yin, S., *et al*., Design of AlN-Based Micro-Channel Heat Sink in Direct Bond Copper for Power Electronics Packaging, *Applied Thermal Engineering*, *52* (2013), 1, pp. 120-129
[3] Lee, P. S., *et al*., Investigation of Heat Transfer in Rectangular Microchannels, *International Journal of Heat Mass Transfer*, *48* (2005), 9, pp. 1688-1704
[4] Zhang, H. Y., *et al*., Single-Phase Liquid Cooled Microchannel Heat Sink for Electronic Packages, *Applied Thermal Engineering*, *25* (2005), 10, pp. 1472-1487
[5] Herwig, H., Mahulikar, S. P., Variable Property Effects in Single-Phase Incompressible Flow through Microchannels, *International Journal of Thermal Science*, *45* (2006), 10, pp. 977-981
[6] Morini, G. L., Scaling Effects for Liquid Flows in Microchannels, *Heat Transfer Engineering*, *27* (2006), 4, pp. 64-73
[7] Husain, A., Kim, K.-Y., Shape Optimization of Micro-Channel Heat Sink for Micro-Electronic Cooling, *IEEE Trans., Component Packaging Technology, 31* (2008), 2, pp. 322-330
[8] Mohammed, H. A., *et al*., Heat Transfer and Fluid Flow Characteristics in Microchannels Heat Exchanger Using Nanofluids: A Review, *Renewable Sustainable Energy Reviews*, *15* (2011), 3, pp. 1502-1512
[9] Lee, J., Mudawar, I., Assessment of the Effectiveness of Nanofluids for Single-Phase and Two-Phase Heat Transfer in Micro-Channels, *International Journal of Heat Mass Transfer*, *50* (2007), 3-4, pp. 452-463
[10] Chein, R., Chuang, J., Experimental Microchannel Heat Sink Performance Studies Using Nanofluids, *Int. Journal of Thermal Sciences*, *46* (2007), 1, pp. 57-66
[11] Ho, C. J., *et al*., An Experimental Investigation of Forced Convective Cooling Performance of a Microchannel Heat Sink with Al_2O_3/Water Nanofluid, *Applied Thermal Engineering*, *30* (2010), 2-3, pp. 96-103
[12] Rimbault, B., *et al*., Experimental Investigation of CuO-Water Nanofluid Flow and Heat Transfer Inside a Microchannel Heat Sink, *International Journal of Thermal Sciences*, *84* (2014), Oct., pp. 275-292
[13] Sakanova, A., *et al*., Optimization and Comparison of Double-Layer and Double-Side Micro-Channel Heat Sinks with Nanofluid for Power Electronics Cooling, *Applied Thermal Engineering*, *65* (2014), 1-2, pp. 124-134
[14] Adham, A. M., *et al*., Optimization of Nanofluid-Cooled Microchannel Heat Sink, *Thermal Science*, *20* (2016), 1, pp. 109-118
[15] Sarkar, J., Transcritical CO_2 Refrigeration Systems: Comparison with Convensional Solutions and Applications, *International Journal of Air-Conditioning & Refrigeration*, *20* (2012), 4, 1250017
[16] Groll, E. A., Kim, J. H., Review of Recent Advances Toward Trans-Critical CO_2 Cycle Technology, *HVAC&R Research*, *13* (2007), 3, pp. 499-520
[17] Ahn, Y., *et al*., Review of Supercritical CO_2 Power Cycle Technology and Current Status of Research and Development, *Nuclear Engineering & Technology*, *47* (2015), 6, pp. 647-661
[18] Sarkar, J., Review and Future Trends of Supercritical CO_2 Rankine Cycle for Low-Grade Heat Conversion, *Renewable & Sustainable Energy Reviews*, *48* (2015), Aug., pp. 434-451
[19] Xu, R., *et al*., A Review on Heat Transfer and Energy Conversion in the Enhanced Geothermal Systems with Water/CO_2 as Working Fluid, *Int. Journal of Energy Research*, *39* (2015), 13, pp. 1722-1741
[20] Sarkar, J., Performance of a Flat Plate Solar Thermal Collector Using Supercritical Carbon Dioxide as Heat Transfer Fluid, *International Journal of Sustainable Energy*, *32* (2013), 6, pp. 531-543
[21] Godec, M., *et al*., CO_2-ECBM: A Review of its Status and Global Potential, *Energy Procedia*, *63* (2014), Dec., pp. 5858-5869

[22] Meylan, F. D., *et al*., CO_2 Utilization in the Perspective of Industrial Ecology, An Overview, *J. CO_2 Utilization*, *12* (2015), Dec., pp. 101-108
[23] Li, Z. H., *et al*., Experimental Investigation of Convection Heat Transfer of CO_2 at Supercritical Pressures in a Vertical Circular Tube, *Exp. Thermal Fluid Science*, *34* (2010), 8, pp. 1162-1171
[24] Jiang, P. X., *et al*., Convection Heat Transfer of Supercritical Pressure Carbon Dioxide in a Vertical Micro Tube from Transition to Turbulent Flow Regime, *Int. J. Heat Mass Transfer*, *56* (2013), 1-2, pp. 741-749
[25] Xu, R. N., *et al*., Experimental Research on the Turbulent Convection Heat Transfer of Supercritical Pressure CO_2 in a Serpentine Vertical Mini Tube, *Int. J. Heat Mass Transfer*, *91* (2015), Dec., pp. 552-561
[26] Ducoulombier, M., *et al*., Charge Reduction Experimental Investigation of CO_2 Single-Phase Flow in a Horizontal Microchannel with Constant Heat Flux Conditions, *Int. J. Refrigeration*, *34* (2011), 4, pp. 827-833
[27] Sarkar, J., *et al*., Transcritical CO_2 Heat Pump Dryer: Part 1. Mathematical Model and Simulation, *Drying Technology*, *24* (2005), 12, pp. 1583-1591

Paper submitted: November 10, 2016
Paper revised: February 17, 2017
Paper accepted: February 17, 2017